Target thickness dependence of Cu K x-ray production for ions moving in thin solid Cu targets*†

R. K. Gardner, Tom J. Gray,‡ Patrick Richard, Carl Schmiedekamp, K. A. Jamison, and J. M. Hall
Department of Physics, Kansas State University, Manhattan, Kansas 66506
(Received 1 October 1976; revised manuscript received 6 December 1976)

Measurements of the target thickness dependence of the target x-ray production yield for incident heavy ions at 1.71 MeV/amu are reported for thin solid Cu targets. The incident ions were F, Al, Si, and S. The charge states of the incident ions were varied in each case to study the target x-ray production for projectiles which have initial charge states q of $q = Z_1$, $q = Z_1 - 1$, and $q < Z_1 - 1$. The target thicknesses were varied from 3 to 85 $\mu g/cm^2$. In each case the Cu K x-ray yields exhibit a complex exponential dependence on target thickness. A three-component model which includes contributions to the target x-ray production due to ions with zero, one, and two K vacancies is developed to describe the observed target K x-ray yields. The three-component model is fitted to the individual data for each projectile, and the cross sections for both the target and projectile are determined. The fits to the target x-ray data give a systematic representation of the processes involved in x-ray production for heavy ions incident on solid targets.

I. INTRODUCTION

In the last decade there has been renewed interest in the study of inner-shell ionization associated with the impact of high-velocity ions. While there is no specific definition of the type of incident ions, they can generally be classified as light ions (e.g., H, He, ...) or heavy ions (e.g., F, Cl, Ar, ...). This classification scheme must necessarily take into consideration the relative atomic numbers of the projectile (Z_1) and the target (Z_2). Generally the theoretical developments have treated the case of ionization by light ions ($Z_1/Z_2 \ll 1$) by considerations based upon direct Coulomb ionization. The plane-wave Born approximation (PWBA),[1] binary-encounter approximation (BEA),[2] and semiclassical approximation (SCA)[3] were developed on this basis. Comparisons of these three theories to K- and L-shell ionization cross sections for H ions over a large range of target atomic numbers and incident ion energies[4] have established that the general features of the experimental data are predicted.

A fundamental feature of the direct-Coulomb theories of inner-shell ionization is that the ionization cross sections should scale as Z_1^2. Experimental investigations using He and Li ions[5-9] to study both K- and L-shell ionization have shown that the cross sections do not scale as Z_1^2. Work by Basbas, Brandt, and Laubert[10] had previously shown that consideration of the effects of perturbations in the target electron-binding energy and deviations from a straight-line trajectory for the projectile gave improved agreement between experimental data and theory for K-shell ionization in the case of H on Al. Their work was based upon the inclusion of binding energy and Coulomb deflection corrections as perturbations to the PWBA. Calculations for ionization by He and Li ions which include these effects (PWBABC) gave improved agreement with target K-shell cross-section data for systems such as He on Cu and Li on Cu.

Experiments which have extended the incident atomic numbers to include C, N, O, F, Si, S, and Cl have been reported.[11-16] The general experimental approach used by the groups involved has been to employ the techniques associated with the studies of inner-shell ionization by light ions in thin solid targets. McDaniel and Duggan[13] have reported K x-ray cross-section data for targets of Ti, Ni, Ge, and Rb with target thicknesses in the range of 5 to 100 $\mu g/cm^2$ for incident ions ranging from H to Cl. Tserruya *et al.*[14] have reported results for S ions on targets of Mn, Ni, Cu, Zn, and Ge having thicknesses <100 $\mu g/cm^2$. Comparisons of these data to theory have been made using the PWBA, PWBABC, and PWBABC with additional corrections for high-energy polarization[13] and relativistic effects.[13,17] Additional comparisons[14] have been made to SCA, BEA, and a vacancy sharing model proposed by Meyerhof.[18] Measurements have shown that the inclusion of the above perturbations to the PWBA gives improved agreement for the light ions (H, He, Li, C, and N). The same type of theoretical calculations result in a significant reduction in the magnitude of the calculated K-shell cross sections for heavy incident ions (F, Si, S, and Cl). The systematics of the disagreement between the calculations and the data for K-shell ionization for heavy ions show that the PWBABC underestimates the measured cross sections by factors ranging from an order of 2–100 depending upon the ion velocity and the target atomic number. In a case such as Cl on Ti[13] the PWBA predictions are within a factor of 2 of the reported cross section measured for a thin solid Ti target while the PWBABC calculations

are a factor of ~100 below the measured x-ray production cross section. Measurements for Cl on Rb[13] show the opposite agreement with the PWBA being a factor of ~30 larger than the measured target K-shell cross section and the PWBABC predictions being a factor of 4 smaller than the reported cross section.

Such variations in the comparisons of direct-Coulomb ionization predictions and experimental data for heavy ions on thin solid targets suggest that there are additional considerations having important theoretical and experimental consequences for understanding the processes involved. Measurements of K-shell x-ray production for symmetric collisions in the cases of Al-Al and Ni-Ni have been reported for thin solid targets by Laubert *et al.*[19] Their work covers the energy range of 0.5–40.0 MeV for Al-Al and 10–63 MeV for Ni-Ni collisions. The work was performed to cover the energy regions wherein the transition from predominately quasimolecular excitation to direct Coulomb excitation should occur. Comparisons of their data to scaled deuteron-deuteron cross sections were made using the procedure reported by Briggs and Macek.[20] Additional calculations for the PWBA and modified PWBA were also reported.[19] The data for Al-Al were predicted by the quasimolecular calculation for incident energies below 3 MeV. However, above 3 MeV the data began to rise above the quasimolecular predictions with increasing ion energy approaching the PWBA predictions. In the case of Ni-Ni the data for the K-shell x-ray production cross section were not represented by the theoretical calculations.

When taken in total the reported measurements and interpretations of target x-ray cross-section data for heavy ions on thin solid targets have not provided to date the information required to allow adequate evaluation of the theoretical models for inner-shell ionization by heavy ions incident at high velocities. Given that the state of comparison between theory and experiment requires improvement, where can other effects that may be of primary importance be brought into consideration? One important contribution may reside in the effects of the K-shell vacancy configurations of the projectile in the solid. Results reported by Winters *et al.*[21] and Mowat *et al.*[22] for heavy ions incident upon gas targets under single-collision conditions has established a charge-dependent effect for the target x-ray production cross sections. The target x-ray production is observed to increase with the increasing charge state of the projectile at a fixed incident energy. Part of the observed increase may be associated with a changing fluorescence yield in the target atom. However, there is a larger enhancement in the target x-ray yield for hydrogenlike and bare projectiles. This suggests that the existence of K vacancies in the projectile is involved in the target K-shell ionization process.

In the dense medium of a solid target the vacancy production and quenching interactions will govern the number of K vacancies in the projectile as it traverses the target. Hence, the existence of fractions of the incident ion beam with one or two K vacancies can be reflected in the target x-ray production cross section. In order to observe such effects two criteria have to be met: (1) there has to be strong coupling between the K vacancies of the projectile and the target K-shell electrons to give rise to enhanced target K-shell ionization, and (2) there has to exist strong coupling of the projectile K shell to the target medium in order to create and/or destroy projectile K-vacancy configurations.

Allison[23] discussed the methods of describing the role of charge-changing collisions for H and He ions moving in gases and presented equations which predict the charge states for two- and three-component systems as a function of target thickness. Betz *et al.*[24] used a two-component model to describe a technique for measuring the lifetimes of atomic states of the projectile moving in a solid. The two component model is structured to account for projectiles moving in the target with or without a single K-shell vacancy. Hopkins[25] has reported the use of the two component model to describe the vacancy fractions of Cl ions moving in thin carbon foils prior to striking a thin Cu layer on the carbon targets. Gray *et al.*[26] have reported an extension of the two component model to describe the target thickness dependence observed in target x-ray production for Cl ions incident on thin solid Cu targets. Similarly Groeneveld *et al.*[27] have studied a two-component model in connection with both projectile and target x-ray production for 10-MeV projectiles on thin Al targets.

It has been established that there exists effects associated with the thickness of the solid target when heavy ions are used to excite target K-shell x rays. The following study was undertaken to assess the magnitude of such effects as a function of Z_1/Z_2, which bring additional dimensions into the considerations of inner shell ionization by heavy ions having both *experimental* and *theoretical* importance. The goals of this work were (1) to extend the considerations of projectile vacancy production and quenching processes to include the existence of the double K-vacancy state in the projectile moving in the target (three-component model), and (2) to provide a systematic study of the production of target K x rays for incident heavy ions having charge states $\leq Z_1$.

II. PROCEDURE

Measurements of Cu K x-ray production cross sections were made for incident F, Al, Si, and S ions on a variety of thin solid Cu targets. Targets ranging in thickness from 3 to 85 $\mu g/cm^2$ were prepared by vacuum evaporation of Cu onto transmission mounted C backings. In addition, a thin layer of Ag($\simeq$50 $\mu g/cm^2$) was evaporated on the back side of each target to allow for normalization to Rutherford scattering. This step was required by the deviations from Rutherford scattering of F on Cu observed in earlier work. The Ag layer also allowed for the reduction in counting time normally required by the thinner Cu targets. The Cu thickness of each target was determined by using a 3-MeV H^+ beam to measure the Cu(p,p)Cu elastic scattering yield at a laboratory angle of 45°. The relative target thicknesses for Cu and Ag were determined in a similar manner. The uncertainty of the measured thickness was $\leq$5%.

Beams of F, Al, Si, and S at 1.71 MeV/amu were obtained from the model EN tandem Van de Graaff accelerator at Kansas State University. The Cu K x rays were detected by a Si(Li) detector at a laboratory angle of 90° with respect to the beam axis, and the scattered ions were detected at a laboratory angle of 30°. The ratio of the number of K x rays, Y_X, to the number of scattered particles, Y_P, was measured simultaneously for each target thicknes and charge state. A greater variety of target thicknesses was obtained by positioning each target at 20°, 30°, and 40° and recording x-ray and particle yields for each angle.

A range of pure charge states for 5^+ to 9^+ F ions, 7^+ to 13^+ Al ions, 8^+ to 14^+ Si ions, and 8^+ to 16^+ S ions was used in the measurements. The higher charge states were obtained by passing the analyzed beam through a carbon-post stripping foil and then selecting the appropriate charge state with magnetic analysis.

The statistical error associated with each experimental point was $\leq$10% and typically <5%. For this data the errors in the absolute magnitude of the measured cross sections were associated with the statistical error and the error in the efficiency of the x-ray detector, which was 10% at 8.9 keV. Thus the absolute error of each data point was at most 15% and typically $\lesssim$10%.

III. THEORY

A proper understanding of target (and projectile) x-ray production cross sections for heavy ions moving in dense media relies on a model which takes into account the K-vacancy states of the projectile as it moves through the medium. It has been shown in a limited number of cases that projectiles with a K vacancy have a substantially different effect on target K-shell ionization cross sections in comparison to those projectiles with no K vacancies. Generally the target cross sections show a relatively large increase in magnitude for hydrogenlike projectiles. This feature of target K-shell ionization by heavy ions suggests that contributions to target x-ray production associated with fractions of the projectile having one or more K-shell vacancies should be included in models which describe the target x-ray production. Such an approach represents a distinct departure from considerations which are the basis of previous measurements and analyses.[13-17]

Previous work by Groeneveld *et al.*[27] presented the development of a two-component model which described projectiles moving in a solid target with and/or without a K vacancy. Results by Gray *et al.*[26] report a similar approach to describe variations in target K x-ray production with target thickness for Cl ions moving in thin solid Cu targets. The basis for the two component model rests on the concept that the fraction of projectiles with no K-shell vacancy, Y_0, and the fraction with one K-shell vacancy, Y_1, are related in such a manner that $Y_0 = 1 - Y_1$. Changes in the relative fractions will then be reflected in the target x-ray production as a function of target thickness. The change of these fractions with the distance, x, which the projectile has traveled in the target has been given[26] by the following rate equation

$$\frac{dY_1}{dx} = \sigma_{01} Y_0 - \sigma_{10} Y_1 , \tag{1}$$

where σ_{if} is the charge-changing cross section, with i representing the number of initial K-shell vacancies in the projectile and f representing the final number of K-shell vacancies in the projectile. The cross section σ_{10}, was assumed to be a sum of the cross section for capture into the K shell of the projectile and the quenching cross section due to the decay of the K-shell vacancy in the projectile. As shown previously when an enhancement in the target x-ray yield is observed for projectiles with a K-shell vacancy compared to projectiles without a K-shell vacancy, it can be assumed that $\sigma_{K1} = \alpha \sigma_{K0}$, where σ_{K1} and σ_{K0} are the target K x-ray production cross sections for projectiles with and without a K-shell vacancy, respectively. Using this assumption along with a weighted average target K x-ray cross section, $\bar{\sigma}_{KX}$, yields

$$\bar{\sigma}_{KX} = \frac{\sigma_{K0}}{T} \int_0^T [1 + (\alpha - 1) Y_1] dx , \tag{2}$$

and thus

$$\bar{\sigma}_{KX}=\sigma_{K0}\left[1+(\alpha-1)\frac{\sigma_{01}}{\sigma}-\frac{\alpha-1}{\sigma T}\left(\frac{\sigma_{01}}{\sigma}-A\right)(1-e^{-\sigma T})\right], \tag{3}$$

where A is the fraction of incident projectiles with a K-shell vacancy and $\sigma=\sigma_{01}+\sigma_{10}$. It is noted for an enhancement of $\alpha=1$ that the averaged target cross section becomes independent of the target thickness, and hence $\bar{\sigma}_{KX}$ is the target K-shell x-ray production cross section. However, for $\alpha>1$ the measured target x-ray yield will depend on the target thickness to varying degrees depending upon the boundary conditions, the ratio of σ_{01}/σ for the projectile, and the strength of the enhancement, α. In the case where the target x-ray yield is measured for projectiles with no K-shell vacancies the appropriate target cross section for comparison to theory is σ_{K0}.

For initial studies of Cl^{q+} ions incident on Cu at 1.71 MeV/amu where only ions of $q\leq Z_1-1$ were available,[26] the two-component model provided an adequate description of the target x-ray yields. However, in the present work for ions lighter than Cl, where $q\leq Z_1$, the two-component model breaks down. The two-component description of $\bar{\sigma}_{KX}$ contains only one exponential term, hence it requires that the target x-ray production cross section either decrease or remain constant as a function of target thickness for incident ions with $q=Z_1-1$. This is clearly not the case for example for 1.71-MeV/amu F^{8+} ions incident on Cu targets (Fig. 1) where $\bar{\sigma}_{KX}$ for Cu increases with increasing target thickness for incident hydrogen-like F ions.

In order to explain this behavior, it is necessary

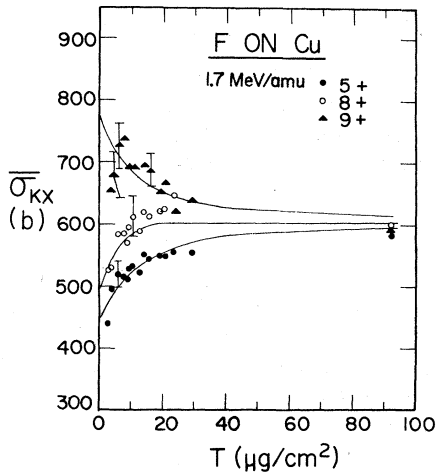

FIG. 1. Thickness dependence of the averaged target cross section, $\bar{\sigma}_{KX}$ for F ions on Cu. The ion charge states 5+, 8+, and 9+ represent the initial conditions for ions with 0, 1, or 2 K-shell vacancies in the incident projectiles.

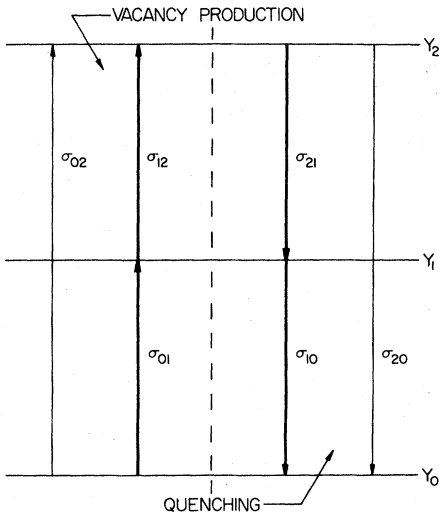

FIG. 2. A representation of the vacancy production and quenching cross sections which govern the K-vacancy fractions for a heavy projectile moving in a dense target. The quantities Y_0, Y_1, and Y_2 represent the states of the projectile with 0, 1, or 2 K vacancies.

to include the possibility of double K-shell vacancies in the projectile. This extension of the two-component model was summarized by Allison.[23] In the three-component model the rate equations describing the projectile vacancies may be written as follows:

$$\frac{dY_2}{dx}=\sigma_{02}Y_0+\sigma_{12}Y_1-(\sigma_{20}+\sigma_{21})Y_2, \tag{4}$$

$$\frac{dY_1}{dx}=\sigma_{01}Y_0-(\sigma_{12}+\sigma_{10})Y_1+\sigma_{21}Y_2, \tag{5}$$

$$1=Y_0+Y_1+Y_2, \tag{6}$$

where the different projectile cross sections are characterized in Fig. 2.

The solutions of these rate equations yield vacancy fractions of the form

$$Y_j=F_{j\infty}+P(i,j)e^{f(\sigma_{if})T}+N(i,j)e^{-f'(\sigma_{if})T},$$

where $F_{j\infty}$ is the equilibrium fraction of ions with j K-shell vacancies, $P(i,j)$ and $N(i,j)$ are functions of the boundary conditions with i equal to the initial number of K-shell vacancies in the projectile and j equal to the number of K-shell vacancies under consideration, and $f(\sigma_{if})$ and $f'(\sigma_{if})$ are functions of the projectile cross sections.[28]

The target x-ray production cross section may be written in terms of the contributions from the individual projectile K-vacancy fractions weighted over the target thickness. However, now there exists not only the single K-shell vacancy enhancement, but also a double K-shell vacancy enhance-

ment, β. Thus,

$$\bar{\sigma}_{KX}=\frac{\sigma_{K0}}{T}\int_0^T [1+(\alpha-1)Y_1+(\beta-1)Y_2]dx\,, \tag{7}$$

where $\sigma_{K1}=\alpha\sigma_{K0}$ and $\sigma_{K2}=\beta\sigma_{K0}$. Note that $\bar{\sigma}_{KX}=\sigma_{K0}$ only for enhancements of $\alpha=1$ and $\beta=1$.

The general solution of this integral may be written as

$$\bar{\sigma}_{KX}=\sigma_{K0}\Big[1+(\alpha-1)\Big(F_{1\infty}+\frac{P(i,1)}{f(\sigma_{if})T}(e^{f(\sigma_{if})T}-1)-\frac{N(i,1)}{f'(\sigma_{if})T}(e^{-f'(\sigma_{if})T}-1)\Big)$$
$$+(\beta-1)\Big(F_{2\infty}+\frac{P(i,2)}{f(\sigma_{if})T}(e^{f(\sigma_{if})T}-1)-\frac{N(i,2)}{f'(\sigma_{if})T}(e^{-f'(\sigma_{if})T}-1)\Big)\Big]\,. \tag{8}$$

The character of the solutions when $\sigma_{if}\approx\sigma_{fi}$ is illustrated in Fig. 3. In general, the target x-ray production cross section for ions with charge $q\leq Z_1-2$ increases toward a saturation value given by

$$\bar{\sigma}_{KX}=\sigma_{K0}[1+(\alpha-1)F_{1\infty}+(\beta-1)F_{2\infty}]\,. \tag{9}$$

For ions with charge $q=Z_1-1$ and $q=Z_1$, $\bar{\sigma}_{KX}$ decreases exponentially with target thickness toward the saturation value. Since the solutions for the three-component model are sums of exponentials, the general character of the solutions strongly depends upon the relative strengths of the vacancy production and quenching interactions for the projectile. Hence, the behavior of the target x-ray production cross section will reflect these relative strengths and the coupling of those vacancies to the target K shell.

IV. EXPERIMENTAL RESULTS AND ANALYSIS

Figure 1 depicts the data for F on Cu with the best fits from the three-component model. These calculations have been performed using a least-squares method which fits all data simultaneously with a single set of parameters, i.e., projectile cross sections, enhancement factors, and σ_{K0}. The general character of the data gives a restricted range of values for the enchancement factors, α and β, and the target K-shell x-ray cross section for a vanishingly thin target, σ_{K0}. Initial estimates of σ_{if} were made and the least-squares fit performed.

The measurements of $\bar{\sigma}_{KX}$ for Al, Si, and S ions on Cu are given in Fig. 4 along with the model fits to the data. In contrast to the F data, the decrease of the target x-ray cross section with thickness for $q=Z_1-1$ illustrates the change in relative K-vacancy populations for the heavier projectiles. In addition, the increase in the enhancement factors, α and β, with increasing atomic number of the projectiles at a fixed value of 1.71 MeV/amu is easily observed.

The K-shell vacancy fractions for the projectile can be calculated as a function of target thickness using the best fit vacancy production and quenching cross sections. In the case of F on Cu the fractions are given in Fig. 5. It is seen that the Y_1 fraction is dominant. This is in agreement with what is to be expected from the results of charge-distribution data for 1.7 MeV/amu F ions in solids. As the atomic number of the projectile is increased the Y_1 fraction decreases while the Y_0 fraction increases at a given depth within the Cu target. This effect, due to the dominance of the projectile quenching cross sections, is easily seen by comparing the F K-vacancy fractions (Fig. 5) to the S K-vacancy fractions (Fig. 6). The equilibration values of Y_0, Y_1, and Y_2 are listed in Table I for each projectile species.

The systematics of the parameters in the expression for $\bar{\sigma}_{KX}$ are shown in Fig. 7. Comparisons to estimates from other sources, where available, are shown. Calculations for the quenching cross sections σ_{10} and σ_{21} have been performed using the

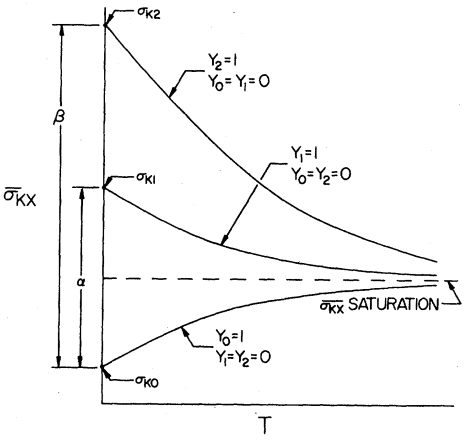

FIG. 3. Qualitative behavior of the three-component model calculations for target x-ray production as a function of target thickness, T. The three curves are labeled by the initial conditions of the incident ion. The calculations represent a typical case where $\sigma_{if}\simeq\sigma_{fi}$. The parameters in this figure are defined within the text.

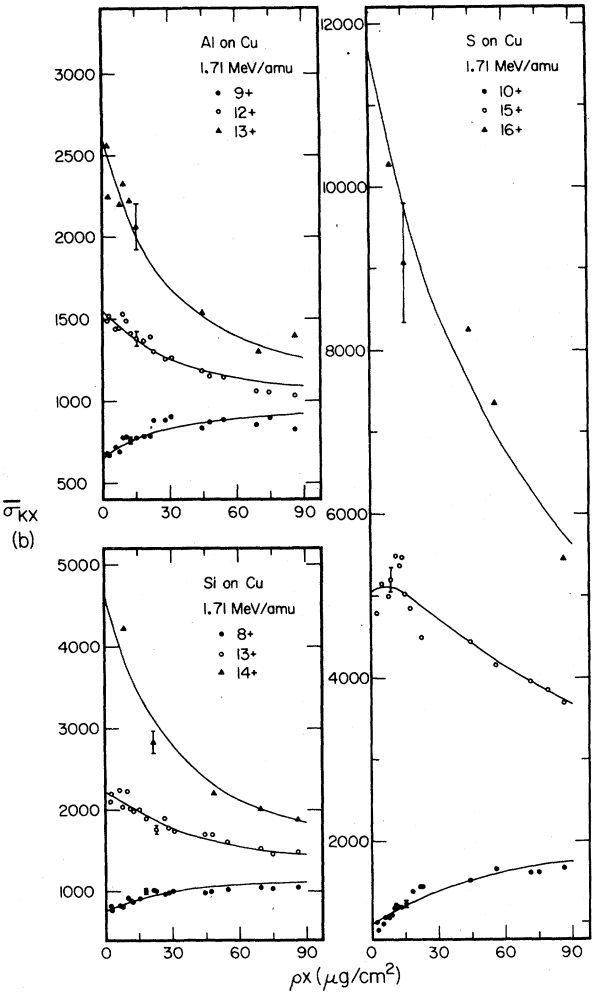

FIG. 4. Experiment results for $\bar{\sigma}_{KX}$ for Al, Si, and S ions on thin solid Cu targets. The solid lines are calculations using the three-component model to simultaneously fit each set of data for a given incident ion species.

Brinkman-Kramers (BK) formulation of charge exchange as given by Nikolaev.[29] These calculations represent the total charge exchange from all shells of the target to the K shell of the projectile. A scaling factor of 1/10 has been introduced to give the calculated estimates for these two cross sections as shown in Fig. 7(a). Previous comparisons between data and BK calculations[30] have shown that scaling factors of 0.1–0.3 are required to give calculated magnitudes which are in agreement with observed experimental data. Contributions to the quenching cross sections due to the decay process described by $\sigma = (nv_1\tau)^{-1}$, where n is the target density and τ is the lifetime of the K vacancy, have

TABLE I. Values of equilibration fraction $F_{j\infty}$ for 1.71-MeV/amu ions incident on Cu targets.

Z_1	$F_{0\infty}$	$F_{1\infty}$	$F_{2\infty}$
9	0.27	0.55	0.18
13	0.70	0.27	0.03
14	0.73	0.24	0.03
16	0.69	0.28	0.03

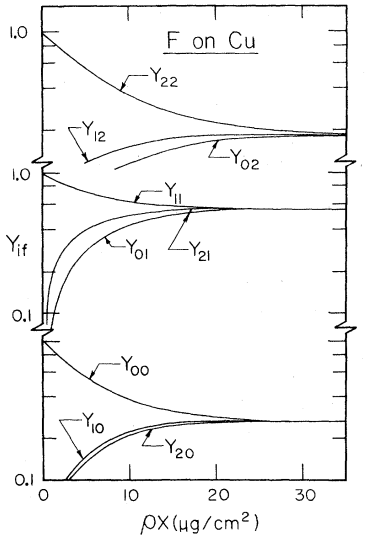

FIG. 5. Projectile K-vacancy fractions as calculated using the projectile cross sections determined from the three-component model fits to $\bar{\sigma}_{KX}$ for F ions incident on Cu at 1.71 MeV/amu. Equilibration fractions are given in Table I.

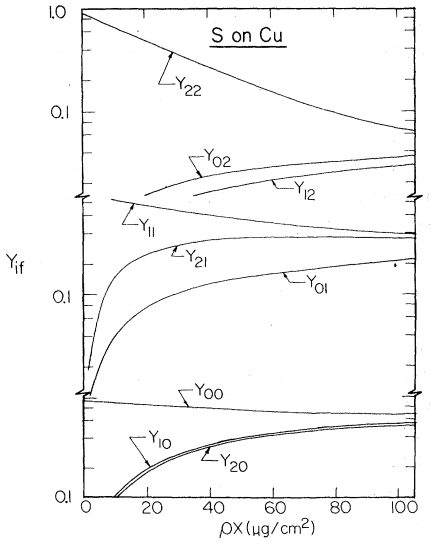

FIG. 6. Projectile K-vacancy fractions as calculated using the projectile cross sections determined from the three-component model fits to $\bar{\sigma}_{KX}$ for S ions incident on Cu at 1.71 MeV/amu. Equilibration fractions are given in Table I.

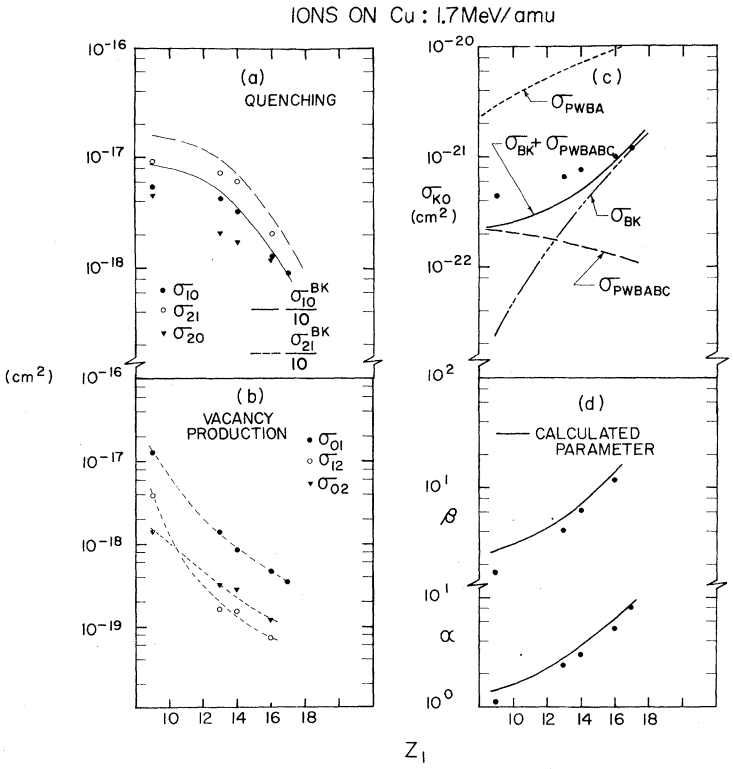

FIG. 7. Systematics of the projectile and target parameters from the fits to the data for $\bar{\sigma}_{KX}$ using the three-component model. Figure 7 (a) and 7 (b) represent the projectile quenching and vacancy cross sections. Figure 7 (c) gives the target cross section, σ_{KO} as defined in the text. The notation σ' denotes the x-ray production cross section where $\sigma'_{PWBA} = \omega_K \sigma_I$ and $\sigma'_{BK} = \omega_K \sigma_{BK}$. Figure 7 (d) gives the values of the enhancement factors α and β with calculations as defined in the text. The data points for Cl on Cu are from Ref. 26.

not been included in the calculated values of σ_{10} and σ_{21} given in Fig. 7(a). The decay component is of order 4×10^{-19} cm^2 for S ions and decreases in relative strength for decreasing atomic number. The projectile quenching cross sections obtained by fitting the target x-ray data with Eq. (8) follow the trends predicted by the BK charge exchange calculations, and hence suggest that the quenching may be described by assuming the dominant process is charge exchange from the target to the K shell of the projectile. The double-quenching cross section σ_{20} follow the general trends given by the single-quenching processes. No attempts at estimating σ_{20} were made in the present work.

The vacancy production cross sections for the projectile K shell are given in Fig. 7(b). The cross sections σ_{01}, σ_{12}, and σ_{02} are representative of interactions which create 1 and 2 K-shell vacancies in the projectile and are thought to contain contributions from both ionization and excitation processes. The short-dashed lines in Fig. 7(b) are eyeguides. Calculations based upon PWBA direct Coulomb ionization of the projectile K shell by Cu for hydrogenlike and heliumlike projectiles give the result that $\sigma_{01} > 2\sigma_{12}$. The values for σ_{01} and σ_{12} extracted from the fits to the target x-ray yield data using Eq. (8) are in general agreement with these crude predictions. The double-vacancy production cross section σ_{02} becomes larger than σ_{12} as Z_1 is increased.

These results do not agree with findings of measurement of single and double electron-loss cross sections which have been reported for O and F ions on dilute gas targets. Works by Macdonald and Martin[31] and Ferguson *et al.*[32] based upon the measurement of charge-state fractions give the result that the single-loss cross sections are larger than the corresponding double-loss cross sections leading to the same final states. Whether or not a direct comparison of such quantities as measured in dilute gases and solids can be made, is not clear. Betz[33] points to the complexity of the problem in his discussion of charge states in solids vs charge states in gases. Further the existence of surface effects for an ion in a foil as discussed by Datz *et al.*[34]; and more recently by Veje[35] further complicate any comparison between information inferred from charge-state distributions and beam-foil related measurements. The influence of cascade transitions and autoionization of the ions between the interaction region and the detection apparatus for charge-state measurements results in additional uncertainties.

In the present measurements the target region serves essentially as a detector of the states of K-shell ionization found in the projectiles. Con-

sider a model for the charge states of an ion moving in a solid target. The charge states are described in terms of the K-shell vacancy fractions and the probabilities for having additional electrons in levels other than the K shell. These additional electrons will be reflected in the charge-state distributions of the ion. However, we have previously shown that they do not have a major influence on the generation of target K-shell x rays for systems like Cl on Cu.[26] From this point of view the charge-state fractions are given by

$$\begin{aligned}
&\phi_{Z_1} = Y_2 g_0 ,\\
&\phi_{(Z_1-1)} = Y_1 g_0 + Y_2 g_1 ,\\
&\phi_{(Z_1-2)} = Y_0 g_0 + Y_1 g_1 + Y_2 g_2 ,\\
&\quad\vdots\\
&\phi_{(Z_1-n)} = Y_0 g_{n-2} + Y_1 g_{n-1} + Y_2 g_n ,
\end{aligned} \tag{10}$$

where ϕ_{Z_i} is the charge-state fraction for an ion with charge Z_i, Y_i are the K-shell vacancy fractions and g_j are the probabilities for having j electrons outside of the K shell. In this model any charge state of the ion can contribute to the production of target x rays through the electron transfer channels associated with the single- and double-K vacancy states of the ion. The measurement of target x-ray production reflects the total contribution from all charge states. Measurements of charge-state distributions downstream from the target have not determined the K-shell vacancy fractions within the target.

The fact that the magnitudes of σ_{02} and σ_{12} from the present work are reversed in comparison with what is observed for charge-state distributions in dilute gases may not be unreasonable. However, there are at present no other independent measurements for such cross sections in solids for F through S ions in the energy range of our measurements. Additionally, there are no reliable theoretical results available for comparison.

It is noted that σ_{02} and σ_{12} are both small in comparison to σ_{01}, σ_{10}, and σ_{21}. In all cases the quenching processes dominate the projectile cross sections. The mathematical structure of Eq. (8) may be somewhat insensitive to the relative values of σ_{02} and σ_{12} because they are small. However the ordering and relative strength of the projectile cross sections for the Y_1 states in comparison to the Y_2 states are reasonable in view of available estimates. Changing the order of σ_{12} and σ_{02} will not modify the main features of the model because of their magnitudes in comparison to the other projectile cross sections. Whether the two cross sections σ_{12} and σ_{02} have physical significance is a question that requires additional investigation. It is certainly not clear that the information derived from charge-state distribution measurements and the results from the present work are simply related or contradictory.

One may compare the values obtained for $\bar{\sigma}_{KX}$ to the predictions of the dynamic screening model proposed by Brandt *et al.*[36] Within that model the target x-ray production cross sections are characterized by the effective charge on the ion as it moves through the solid. In the limit of a vanishingly thin target the charge of the ion is its incident charge state. Hence, the dynamic screening model predicts that

$$\beta \sim \left(\frac{Z_1}{Z_1-3}\right)^2 \quad \text{and} \quad \alpha \sim \left(\frac{Z_1-1}{Z_1-3}\right)^2 . \tag{11}$$

Evaluation of these expressions for S on Cu gives $\alpha = 1.3$ and $\beta = 1.51$. These are to be compared with the experimentally determined values of $\alpha = 5.1$ and $\beta = 11.6$. Application of the dynamic screening model to the data for Al and Si leads to the same kinds of disagreement. In the case of F the dynamic screening model gives results which agree with the present results for α and β. However, this is a case where the coupling between the target and projectile K shell is weak and hence the enhancements are predicted to be small. In view of the divergence between the predictions of the dynamic screening model and the data as Z_1 increases from F to S it is proposed that the dynamic screening model is not appropriate to the description of target K x-ray production.

The experimental values of σ_{K0} are given in Fig. 7(c) for the incident ions F, Al, Si, S, and Cl at 1.7 MeV/amu. Plane-wave Born approximation (PWBA) calculations for σ_{K0} are shown in the figure. The PWBA calculations overestimate the cross sections by an order of magnitude. This trend is in agreement with the systematics from earlier work[16] for lighter ions in elements in the range of Cu. In order to obtain an estimate of σ_{K0} it is assumed that there are two mechanisms for creating K vacancies in the target; direct Coulomb ionization and charge exchange from the 1s shell of the target to projectile states having $n \geq 2$. Brinkman-Kramers calculations for the charge-exchange component were scaled by the factor of $\frac{1}{10}$ and multiplied by the atomic value of ω_K for Cu to give the cross section $\omega_K \sigma_{BK}$. Calculations for the direct Coulomb contribution were taken from Brandt and Lapicki[37] for the PWBABC. As has been shown earlier[13,16] the binding energy correction causes a large reduction in the calculated cross sections. The value of σ_{K0} was then taken to

be

$$\sigma_{K0} = (\sigma_{\mathrm{PWBABC}} + \sigma_{\mathrm{BK}})\omega_K . \tag{12}$$

The individual contributions for $\omega_K\sigma_{\mathrm{BK}}$ and $\omega_K\sigma_{\mathrm{PWBABC}}$ are shown in Fig. 7(c). The estimates for σ_{K0} as described above give qualitative agreement with the experimental data.

The parameters α and β obtained from the data are given in Fig. 7(d). The calculated values of α and β are based upon the following equations

$$\alpha = \frac{\sigma_{K0} + w\omega\pi R^2}{\sigma_{K0}} \tag{13}$$

and

$$\beta = \frac{\sigma_{K0} + 2w'\omega\pi R^2}{\sigma_{K0}} \tag{14}$$

where ω is the neutral atom fluorescence yield for Cu. Estimates[38] of the effects of multiple ionization on ω for Cu show that the change in ω should be $\lesssim 15\%$. Hydrogenlike and heliumlike binding energies[39] were used in the calculation of w' and w, the Meyerhof vacancy transfer probabilities,[18] for the $q = Z_1$ and $q = Z_1 - 1$ charge states of the incident ion. The values of R were taken from the peaks of the dynamic coupling elements as given by Taulbjerg *et al.*[40] The agreement between the data and predictions of the proposed model for α and β support the hypothesis that the $1s$-to-$1s$ vacancy transfer mechanism is a plausible interaction by which the x-ray production cross section is enhanced for the bare and hydrogenlike incident ions.

V. CONCLUSION

In summary, the systematics of thin solid target K x-ray production for heavy ions incident on Cu have been illustrated. The dependence of the target x-ray yield on the target thickness and projectile atomic number establishes the need for a model which includes effects for K-vacancy fractions in the projectile and the coupling of those vacancies to the target K shell. The three-component model which is presented can satisfy the requirements for a more definitive approach to the design and execution of experiments and the interpretation of data for x-ray production in the case of high velocity heavy ions incident upon solid targets. Clearly previous solid target x-ray production cross sections from heavy ion bombardment at high velocities which do not include the effects established in the present work may not provide an adequate basis for direct testing of either the direct Coulomb or quasimolecular theories for inner-shell ionization. The complexity of x-ray production for heavy ions incident on solids and the lack of sufficient data for projectile-vacancy production and quenching processes suggest that correcting existing data derived from a single-target thickness measurements would be difficult if not impossible.

The systematics of the vacancy production cross sections for the projectile represents an area which is in need of further investigation. It is not clear that the charge-changing cross sections obtained from the measurements of charge-state fractions are directly comparable to the K-vacancy production cross section derived from the three-component model. The model is sensitive to the existence of a single- or double-vacancy state in the K-shell of the projectile. No distinction is made between excitation or ionization which leads to the creation of a projectile K vacancy. Further tests of the three-component model may provide the basis for understanding the nature of the projectile-vacancy production processes in solids.

In the case of x-ray production for heavy ions incident upon solid targets the comparison of theoretical calculations for inner-shell ionization should be made to experimental cross sections measured for a vanishingly thin target. The relevant target cross sections for such comparisons are σ_{K0}, σ_{K1}, and σ_{K2} for incident projectile charge states of $Z_1 - 3$, $Z_1 - 1$, and Z_1, respectively. Measurements of heavy-ion target x-ray production on targets having a thickness of the order $\gtrsim 10$'s $\mu\mathrm{g/cm}^2$ result in cross sections which can deviate significantly from the results required for comparisons to existing inner-shell ionization theories.

ACKNOWLEDGMENTS

The authors wish to acknowledge the helpful discussions and suggestions connected with the present work by C. L. Cocke and J. H. McGuire. The help of R. E. Rose in phases of data acquisition for this work is also acknowledged.

---

*Work supported in part by the Division of Physical Research, U.S. Energy Research and Development Administration and the Faculty Research Fund, North Texas State University.

†This paper is based on material presented at the International Conference on the Physics of X-Ray Spectra, National Bureau of Standards, Gaithersburg, Md., 1976; see Program and Extended Abstracts.

‡On leave from North Texas State University, Denton, Texas.

[1] G. S. Khandelwal, B. H. Choi, and E. Merzbacher, At. Data 1, 103 (1969).

[2]J. D. Garcia, E. Gerjuoy, and J. E. Welker, Phys. Rev. 165, 66 (1968).
[3]J. Bang and J. M. Hansteen, K. Dan. Vidensk. Selsk. Mat.-Fys. Medd. 31, No. 13 (1959).
[4]See for example the review papers by J. D. Garcia, R. J. Fortner, and T. M. Kavanagh, Rev. Mod. Phys. 45, 111 (1973); Patrick Richard, *Atomic Inner-Shell Processes*, edited by Bernd Crasemann (Academic, New York, 1975), p. 73.
[5]C. N. Chang, J. F. Morgan, and S. L. Blatt, Phys. Rev. A 11, 607 (1975).
[6]F. D. McDaniel, T. J. Gray, R. K. Gardner, G. M. Light, J. L. Duggan, H. A. Van Rinsvelt, R. D. Lear, G. H. Pepper, J. W. Nelson, and A. R. Zander, Phys. Rev. A 12, 1271 (1975).
[7]Tom J. Gray, G. M. Light, R. K. Gardner, and F. D. McDaniel, Phys. Rev. A 12, 2393 (1975).
[8]F. Hopkins, R. Brenn, A. R. Whittemore, J. Karp, and S. K. Bhattacherjee, Phys. Rev. A 11, 916 (1975).
[9]H. Tawara, Y. Hachiya, K. Ishii, and S. Morita, Phys. Rev. A 13, 572 (1976).
[10]G. Basbas, W. Brandt, and R. Laubert, Phys. Rev. A 7, 983 (1973).
[11]R. P. Chaturvedi, J. L. Duggan, T. J. Gray, C. C. Satchleben, and J. Lin, Twenty-Second Annual Denver X-ray Conference, 1973, Denver, Colo.
[12]R. M. Wheeler, R. P. Chaturvedi, J. L. Duggan, J. Tricomi, and P. D. Miller, Phys. Rev. A 13, 958 (1976).
[13]F. D. McDaniel and J. L. Duggan, *Beam-Foil Spectroscopy*, edited by I. A. Sellin and D. J. Pegg (Plenum, N.Y., 1975), p. 519.
[14]I. Tserruya, R. Schulé, H. Schmidt-Böcking, and K. Bethge, Z. Phys. A 277, 233 (1976).
[15]F. D. McDaniel, J. L. Duggan, J. Tricomi, P. D. Miller, K. A. Kuenhold, F. Elliott, J. Lin, R. M. Wheeler, and R. P. Chaturvedi, Bull. Am. Phys. Soc. 21, 650 (1976).
[16]T. J. Gray, P. Richard, R. Kauffman, T. C. Holloway, R. K. Gardner, G. M. Light, and J. Guertin, Phys. Rev. A 13, 1344 (1976).
[17]T. L. Hardt and R. L. Watson, Phys. Rev. A 7, 1917 (1973).
[18]W. E. Meyerhof, Phys. Rev. Lett. 31, 1341 (1973).
[19]R. Laubert, H. Haselton, J. R. Mowat, R. S. Peterson, and I. A. Sellin, Phys. Rev. A 11, 135 (1975).
[20]J. S. Briggs and J. H. Macek, J. Phys. B 6, 982 (1973).
[21]L. Winters, M. D. Brown, L. D. Ellsworth, T. Chaio, E. W. Pettus, and J. R. Macdonald, Phys. Rev. A 11, 174 (1975).
[22]J. Richard Mowat, I. A. Sellin, P. M. Griffin, D. J. Pegg, and R. S. Peterson, Phys. Rev. A 9, 644 (1974).
[23]S. K. Allison, Rev. Mod. Phys. 30, 1137 (1958).
[24]H. D. Betz, F. Bell, H. Panke, G. Kalkoffen, M. Solz, and D. Evers, Phys. Rev. Lett. 30, 358 (1973).
[25]F. Hopkins, Phys. Rev. Lett. 35, 270 (1975).
[26]T. J. Gray, P. Richard, R. K. Gardner, K. A. Jamison, and J. M. Hall, Phys. Rev. A 14, 1333 (1976).
[27]K. O. Groeneveld, B. Kolb, J. Schader, and K. D. Sevier, Z. Phys. A 277, 13 (1976).
[28]The notation used in connection with the three compound model is taken from Ref. 23.
[29]V. S. Nikolaev, Zh. Eksp. Teor. Fiz. 51, 1203 (1966) [Sov. Phys.-JETP 24, 847 (1967)].
[30]A. M. Halpern and J. Law, Phys. Rev. Lett. 31, 4 (1973).
[31]J. R. Macdonald and F. W. Martin, Phys. Rev. A 4, 1965 (1971); and F. W. Martin and J. R. Macdonald, Phys. Rev. A 4, 1974 (1971).
[32]S. M. Ferguson, J. R. Macdonald, T. Chiao, L. D. Ellsworth, and S. A. Savoy, Phys. Rev. A 8, 2417 (1973).
[33]H. D. Betz, Rev. Mod. Phys. 44, 465 (1972).
[34]S. Datz, B. R. Appleton, J. A. Biggerstaff, M. D. Brown, H. F. Krause, C. F. Moak and T. S. Naggle, in *Atomic Collisions in Solids*, edited by S. Datz, B. R. Appleton, and C. D. Moak (Plenum, New York, 1975), Vol. 1, pp. 63–73.
[35]E. Veje, Phys. Rev. A 14, 2077 (1976).
[36]W. Brandt, R. Laubert, M. Mourino, and A. Schwarzschild, Phys. Rev. Lett. 30, 358 (1973).
[37]W. Brandt and G. Lapicki, Phys. Rev. A 10, 474 (1974).
[38]F. D. Larkins, J. Phys. B 4, L29 (1971).
[39]C. E. Moore, NSRDS-NBS No. 34 (1970).
[40]K. Taulbjerg, J. Vaaben, and B. Fastrup, Phys. Rev. A 12, 2325 (1975).